Hydraulic fracturing induced hybrid earthquakes in the Montney Formation, British Columbia, Canada may mark the transition from aseismic slip near the wellbore to seismic slip at greater distances

Hongyu Yu[1*], Rebecca M. Harrington[2], Honn Kao[1,3], Yajing Liu[4], and Bei Wang[1,3]

[1]Geological Survey of Canada, Sidney, British Columbia, Canada, V8L 5T5 [2]Institut für Geologie, Mineralogie und Geophysik, Ruhr-Universität Bochum, Bochum, Germany, 44801.
[3]School of Earth and Ocean Sciences, University of Victoria, Victoria, British Columbia, Canada, V8W 3V6. [4]Earth and Planetary Sciences Department, McGill University, Montreal, Quebec, Canada, H3A 0E8.

Abstract ERE6.2-4544

Summary

Aseismic slip loading is recently proposed as a complimentary mechanism for moderate earthquakes (M3+) that are induced at the onset of hydraulic fracturing (HF) simulations, located several kilometers from the wellbore. However, aseismic/slow slip signals linked to fluid-injection-induced earthquakes remain largely undocumented to date. Here we report a new type of seismic signal near injection wells consisting of impulsive broadband onsets followed by protracted low frequency ringing (hybrids). Hybrids are characterized by broader pulses and lower stress drops compared to ordinary induced earthquakes, suggesting slower rupture. Hybrids could thus represent the seismic manifestation of low-frequency earthquakes that bridge the slow (aseismic) slip inferred by recent modeling and observations near the wellbore to seismic slip at greater distances.

Study area and Dataset

The Montney Play is one of the most active oil and gas production areas in Canada. Since the start of hydraulic fracturing (HF) activities in 2008, it has experienced a drastic increase of local seismicity, including 3 significant (M4.5+) earthquakes (Fig. 1A).

With the express purpose of capturing the seismicity associated with a hydraulic fracturing treatment in the Montney Play, eight broadband seismograph stations were deployed surrounding a HF well pad during May 28 – Oct 15, 2015 (MG01-08; Fig. 1B).

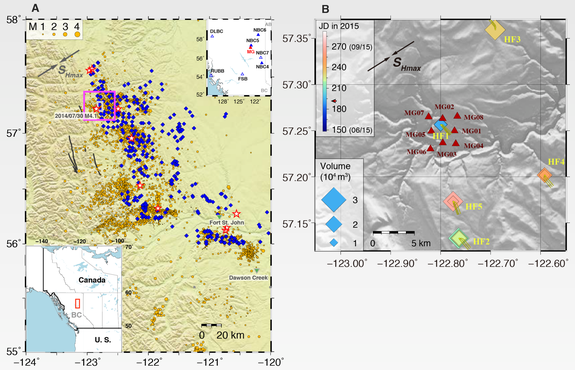

Fig. 1 | Study area. (**A**) Hydraulic fracturing activity (Blue) and seismicity (Yellow) during 2014-2016. Stars: M 4-5 earthquakes since 2008. Insets: the Montney Play; Solid/empty triangles: regional stations with/without clear phase arrivals of hybrids). **(B)** Distribution of stations MG01-08.

References

S. Ide, G. C. Beroza, D. R. Shelly, T. Uchide, A scaling law for slow earthquakes. *Nature*, **447**(7140), 76 (2007).

S. Ide, K. Imanishi, Y. Yoshida, G. C. Beroza, D. R. Shelly, Bridging the gap between seismically and geodetically detected slow earthquakes. *Geophys. Res. Lett.*, **35**, L10305 (2008).

S. Michel, A. Gualandi, J. P. Avouac, Similar scaling laws for earthquakes and Cascadia slow-slip events. *Nature*, **574**(7779), 522-526 (2019).

Features of hybrid signals

Unique hybrid-frequency waveforms (Hybrids; Fig. 2):

- ✓ Impulsive broadband onsets
- ✓ Broader body wave arrival pulses compared to standard events
- ✓ Protracted low-frequency ringing (<5-7 Hz; ~10 s)

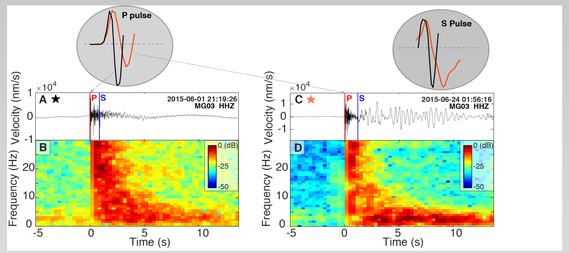

Fig. 2 | Comparison between representative examples of standard induced (A-B) and hybrid events (C-D). Both have ~M_W 1.5 with source station distances of 1.32 km vs. 1.65 km.

Hybrids outline a planar structure

A total of 31 hybrid detections with 28 well-constrained hypocenters. Two hybrid groups (Fig. 3A)

- ✓ In close proximity to the horizontal wellbore
- ✓ Southern cluster: ~2 km south of the wellbore
  - Best fit by a plane (blue shaded area) with average distance of 0.14 km ± 0.10 km.
  - High waveform similarity (Fig. 3B)
  - Consistent origin hours (Fig. 3D)

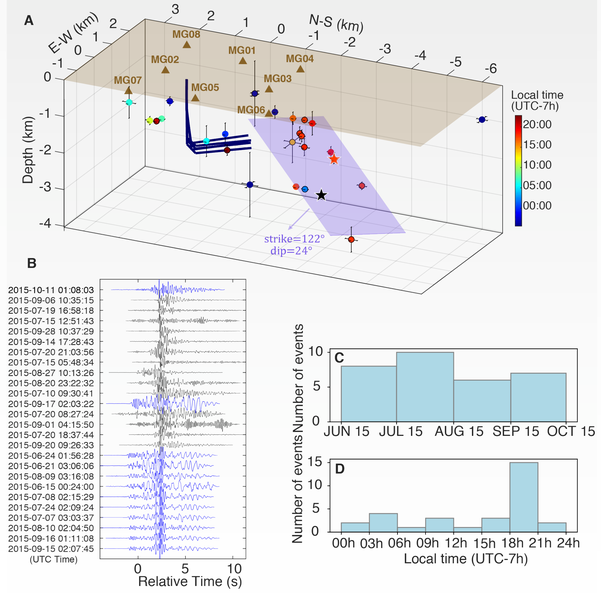

Fig. 3 | Spatial and temporal distribution of hybrid events. (**A**) 3D hybrid distribution. Dots: 28 relocated hybrids. **(B)** Alignment of hybrids signals on MG08 (HHE). Blue: the southern hybrid cluster. (**C**) Histogram of origin time. (**D**) Histogram of origin hour.

Hybrids source mechanisms

What physical mechanism could explain the hybrid waveforms?

Two commonly proposed mechanisms of volcanic hybrids:

- ✓ coupling between turbulent flow and the sides of an open crack
- ✓ stick-slip rupture with low rupture velocity and/or strongly attenuated travel paths

One way to rule out one of the above is to check the consistency of the **size-duration scaling** between the broadband onset and low-frequency ringing portion of hybrid waveforms.

Broadband onsets: origin from slower brittle ruptures similar to LFEs (Fig. 4):

- Self-similarity in stress drop ($M_0 \sim f_c^{-3}$).
- Low stress drops compared to ordinary induced earthquakes (0.29 MPa vs. 4.86 MPa) .
- Stress drop values of the southern cluster (~1 MPa) are generally higher than hybrid close to the wellbore (~0.1 MPa).
- Linked across the broad scale, hybrids are consistent with the linear moment-duration scaling ($M_0 \propto T$) inferred for a broad range of slow slip phenomena (Fig. 5).

Low-frequency ringing depends on the ray path:

- Apparent duration varies consistently with the path effects, which may stem from velocity heterogeneity near the wellbores (Fig. 6).
- A positive correlation between hypocentral distance and apparent duration holds for the station that is least likely affected by velocity heterogeneity along its travel path (MG08; Fig. 7).

Broadband onset size-duration scaling similar to LFEs

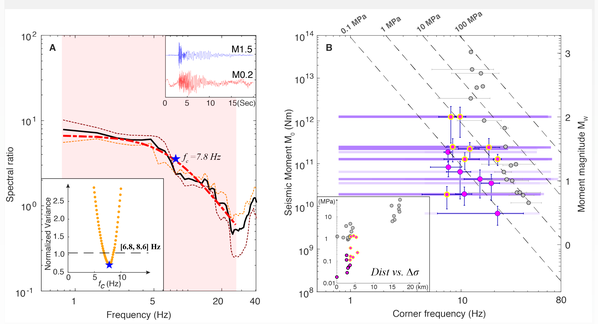

Fig. 4 | Source parameter estimates of broadband onset. (**A**) Example of spectral ratio fitting between an event pair. Stacked event pair spectral ratio (Black) is obtained from records at MG05 (dark red) and MG06 (orange), fitted by a Brune model (Red) with optimal f_c shown. (**B**) Scaling between corner frequency f_c and seismic moment M_0. Pink/gray dots: f_c and M_0 estimated from spectral ratio fitting of S-phase for hybrids/ordinary induced events constrained using the same approach and dataset. Yellow rings indicate hybrids from southern cluster. Horizontal error bars: frequency band with 5% increase of fit variance. Vertical error bars: standard error of low-frequency amplitude variance. Purple transparent bars: frequency band used for fitting. Inset: stress drop as a function of well distance.

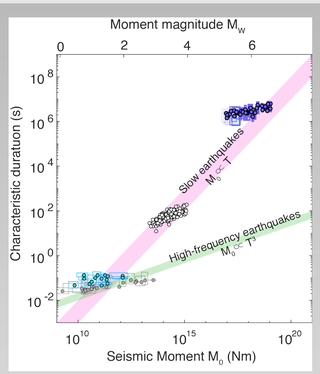

Fig. 5 | Moment-duration scaling. Pink/green bars: proposed moment-duration scaling for slow and ordinary (fast) earthquakes *(Ide et al., 2007)*. Light blue/gray dots with rectangles: hybrids/ordinary events in this study with uncertainties indicated in Fig. 3B. Duration is constrained using the P/S-wave spectral corner frequency. White dots: low-frequency earthquakes in Kii Peninsula, Japan *(Ide et al., 2008)*; purple dots: slow-slip events in Cascadia *(Michel et al., 2019)*.

Low-frequency ringing: ray path dependency

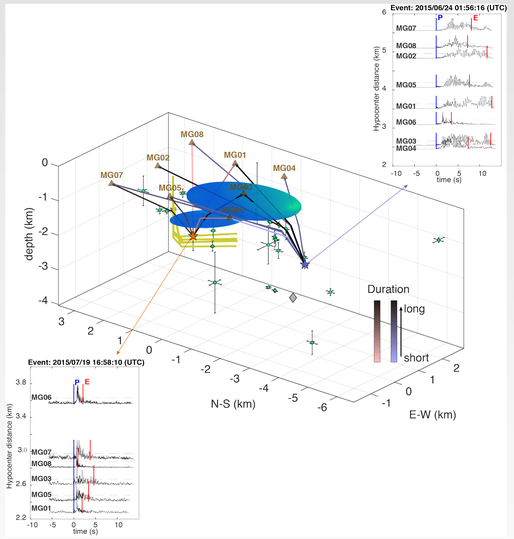

Fig. 6 | Conceptual 3D plot of ray travel path through velocity structure heterogeneities. Green dots: hybrid events. Solid curve: ray path geometry. Blue ellipsoids: volumes of material with velocity heterogeneities. Thick yellow curve: hydraulic fracturing well geometry.

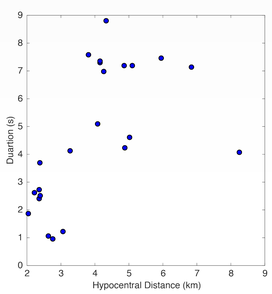

Fig. 7 | Distance-duration scaling station MG08. Each blue dot represents one hybrid event. The duration follows a linear fit given by Duration (s) = 1.30 × Distance (km) - 0.21, with a coefficient of determination (R-squared) value equal to 60.4%, i.e., ~60% of the variation in duration at MG08 could be explained by the hypocentral distance in the linear regression model.